Evolution of solitons in magnetic thin films

C. E. Zaspel,[1] J. H. Mantha,[1] Yu. G. Rapoport,[2] and V. V. Grimalsky[3]
[1]*Department of Environmental Sciences, University of Montana/Western, Dillon, Montana 59725*
[2]*Department of Astronomy and Space Physics, Kiev University, 252022 Kiev, Ukraine*
[3]*National Institute for Astrophysics, Optics and Electronics, ZP 72000, Puebla, Pue., Mexico*
(Received 6 February 2001; published 23 July 2001)

Localized magnetostatic wave pulses propagating in a magnetic thin film can be modeled by a nonlinear Schroedinger equation, which has stable envelope soliton solutions. When the wave velocity depends also on the wave amplitude it is necessary to add a self-steepening term to the evolution equation. However, when this is done the original envelope will evolve from a symmetric structure into an asymmetric structure as a direct result of the self-steepening term. An approximate time envelope shape is analytically calculated to obtain the time dependence of the asymmetry, and numerical simulations also indicate similar temporal development. Finally, the analytical calculation is compared with previous experimental pulse shapes obtained during propagation in yttrium iron garnet thin films.

DOI: 10.1103/PhysRevB.64.064416 PACS number(s): 75.70.Ak, 05.45.Yv, 42.65.Tg

I. INTRODUCTION

Microwave envelope solitons can be produced in magnetic thin films such as yttrium iron garnet (YIG) by use of a simple delay-line setup. In this system a bright soliton evolves when a finite duration pulse on a microwave frequency carrier wave is launched from a microstrip antenna attached to the film, and it is detected at a second microstrip antenna a few millimeters down the film. In addition to the potential applications in the area of microwave signal processing, these experiments[1–3] provide useful tests of the theory of microwave propagation and soliton formation in magnetic films. In the development of theories a single pulse has a frequency spectrum of width $\delta\omega$ on a carrier frequency, ω_0 defining ''slow'' and ''fast'' characteristic times, respectively. If it is assumed that $\delta\omega \ll \omega_0$ then one can describe the dynamics of propagation in terms of the ''slow'' characteristic time leading to the envelope approximation giving the nonlinear Schroedinger (NLS) equation describing the evolution of the pulse. The NLS equation is one of the few equations that can be solved[4] by the inverse scattering method so it is possible to find a solution from an arbitrary initial pulse shape, and a comparison can be made with experimental results using YIG films. In general, experiments can be explained by use of the NLS equation, and particular examples are soliton formation[5] and soliton decay[6] resulting from dissipation in YIG films.

There are situations when the envelope approximation is not valid and the NLS model is not expected to be applicable; in particular, this can occur if the pulse is narrow ($\delta\omega \approx \omega_0$) or if the pulse amplitude is large. The usual strategy in these situations has been the addition of higher-order terms in the NLS equation such as higher-order linear and nonlinear dispersion resulting in a higher-order nonlinear Schroedinger (HONLS) equation. However, if the pulse is too narrow (the order of the carrier wavelength) this approximation will not be adequate[7] no matter how many terms are included. Here we are interested in the intermediate case when the envelope approximation is still valid, but the higher-order terms can also have an effect on the pulse shape. There are analytic solutions[8–11] of the HONLS equation with third-order dispersion and first-order nonlinear dispersion (or self-steepening) as the higher-order terms. In order for multisoliton solutions to exist, it has been shown[8–10] that the coefficients in the HONLS model must satisfy certain relations, but this probably will not be the case in physical systems so these solutions are only of mathematical interest. On the other hand, the single soliton solutions can exist for arbitrary values of the coefficients, except for sign constraints, so these might be more applicable. However, there are no free parameters in these solutions, so again they are too restricted to be useful. The HONLS equation with the self-steepening term only has soliton solutions[12] and it has also been used to analytically model[13,14] shock development. However, it was recently shown[15] that there was an error in this analytical work resulting from inconsistent solution of an overdetermined set of equations. There are also some interesting recent numerical studies[16,17] of this system, showing that a symmetric pulse will evolve into one or more solitons as well as a linear wave train. This can be a noticeable effect in optical fibers, but in YIG films the propagation distance is too short for the linear wave train to be noticeable.

Usually it is expected that the effects resulting from the higher-order terms will be small; nevertheless, it is of interest to experimentally observe such effects to test the limits of the NLS model. Previous experiments have shown that the soliton velocity has a weak dependence on the input pulse power, and this was subsequently explained[18] through the addition of higher-order linear and nonlinear dispersion in the NLS equation. To find other effects that can be explained through higher-order terms, we will investigate the short-time evolution of a pulse in a YIG film. To accomplish this, approximate analytic solutions of a HONLS equation will be obtained, which will be more general and applicable than the known exact solutions. First, a temporal series solution is developed so that the time evolution of an initial pulse can be determined. Using this solution the change in shape of a pulse can actually be calculated which is an effect that cannot be studied through the soliton solutions of the HONLS

equation. The calculated pulse shape is compared with numerical simulation of the same equation to indicate that this solution is stable and general. The overall objective of this research is to provide methods to experimentally detect the effects arising from the higher-order terms. Therefore the calculated pulse shapes are compared with pulse shapes obtained during propagation in YIG films and it is shown that the higher-order terms can, indeed, have a measurable effect on microwave pulse propagation.

II. SOLUTION OF THE MODEL EQUATION

The time evolution of a pulse is determined from the standard nonlinear Schrödinger equation with a higher-order self-steepening term as a perturbation. This term is the direct result of an amplitude dependent group velocity and it is expressed as the last term in the following HONLS equation:

$$i\varphi_t+\frac{D}{2}\varphi_{xx}-N|\varphi|^2\varphi-iQ(|\varphi|^2\varphi)_x=0, \tag{1}$$

where the complex envelope function $\varphi(x,t)$ specifies a pulse traveling in the x direction and the subscripts indicate partial differentiation. The coefficients in Eq. (1) are obtained from derivatives of the magnetostatic wave dispersion relation $\omega(k,|\varphi|^2)$, where $D=\partial^2\omega/\partial k^2$ is the dispersion coefficient, $N=\partial\omega/\partial|\varphi|^2$ is the nonlinear coefficient, and $Q=\partial N/\partial k$ is the nonlinear dispersion coefficient. All coefficients are evaluated at the carrier wave number and for $|\varphi|^2=0$. We begin by expressing the complex envelope function as

$$\varphi(x,t)=u(x,t)e^{i\sigma(x,t)}, \tag{2}$$

where u and σ are real functions. Then substitution of Eq. (2) into the HONLS equation and separately equating the imaginary and real parts to zero gives the two equations

$$u_t+\frac{D}{2}(u_{xx}+2u_x\sigma_x)+3Qu^2u_x=0, \tag{3a}$$

$$-u\sigma_t+\frac{D}{2}(u_{xx}-u\sigma_x^2)-(N+Q\sigma_x)u^3=0. \tag{3b}$$

Next it is possible to express Eqs. (3a) and (3b) in conservation law form,

$$(u^2)_t+(\psi u^2)_x=0, \tag{4a}$$

$$\psi_t+\left(\frac{\psi^2}{2}+A(\psi)\right)_x, \tag{4b}$$

where the function ψ is defined by $\psi=3Qu^2/2+D\sigma_x$, $A(\psi)$ is an arbitrary function, and all functions must be related by

$$\frac{D^2u_{xx}}{2u}-NDu^2+\frac{Q^2}{4}u^4-\frac{Q}{2}\psi u^2-A(\psi)=0. \tag{5}$$

At this point we have three equations and three unknowns, but the third unknown function is itself a function of ψ so the main problem here is the determination of A so that all three equations will be consistent. This will be done by development of a temporal series solution for u so that the time evolution can be determined from an arbitrary initial envelope shape.

The first step in this process is the development of a series solution for ψ, which will be general at this stage because Eq. (4b) has the soft solution $\psi=g(x-\psi t-A_\psi t)$ where g is still an arbitrary function. Using the soft solution it is easy to derive the following series for ψ if the form is assumed for the function $A(\psi)=a_0+a_1\psi+a_2\psi^2+\ldots$,

$$\psi=g+\psi_1 t+\psi_2 t^2=0, \tag{6}$$

where $\psi_1=-(a_1+\alpha_2 g)g_x$, $\psi_2=(a_1+\alpha_2 g)[g_{xx}(a_1+\alpha_2 g)+\alpha_2 g_x^2]/2$, and $\alpha_2=1+2a_2$. This is the solution of Eq. (4b) and it is next necessary to consistently solve Eqs. (4a) and (5) to obtain u in the form of a series.

Next it is assumed that u is expressed as the series

$$u=u_0+\varepsilon_1 t+\varepsilon_2 t+\ldots, \tag{7}$$

where u_0 is the initial form of the pulse and the other coefficients are in general dependent on x. To find these coefficients Eqs. (6) and (7) are substituted into Eq. (4a), it is assumed that g has the form $g=\alpha+\beta u_0^2$, and Eq. (4a) is written in series form. The coefficients of each power of t are then equated to zero to obtain the set of equations for the coefficients ε_n,

$$u_{0t}+\alpha u_{0x}+2\beta u_0^2u_{0x}+\varepsilon_1=0, \tag{8a}$$

$$\varepsilon_{1t}+\alpha\varepsilon_{1x}+\beta u_0^2u_{0x}+\psi_1u_{0x}+\tfrac{1}{2}u_0\psi_{1x}+\beta u_0u_{0x}\varepsilon_1+2\varepsilon_2=0 \tag{8b}$$

corresponding to the coefficients of the t^0 and t^1 terms, respectively. It is remarked that the lowest order Eq. (8a) is used to obtain ε_1 and the higher-order equations can be used to obtain the other coefficients.

The final step is the solution of Eq. (5), which is done by substitution of the series for ψ and u into Eq. (5) with the values for ε from Eqs. (8). Again, this will give a power series in t with complicated coefficients that will be functions of u_0, and when the coefficients are equated to zero we obtain the set of equations

$$u_{0xx}+\left(\frac{Q^2}{2D^2}+\frac{Q\beta}{D^2}-\frac{2a_2\beta^2}{D^2}\right)u_0^5-\left(\frac{2N}{D}+\frac{2a_1\beta}{D^2}\right)u_0^3-\frac{2a_0}{D^2}u_0=0, \tag{9a}$$

$$\frac{D^2}{2}\varepsilon_{1xx}+\left(3ND+\frac{5}{4}Q^2u_0^2+\frac{3}{2}Qg\right)u_0^2\varepsilon_1+\left(\frac{Q}{2}u_0^2-a_1-2a_2g\right)u_0\psi_1-(a_0+a_1g+a_2g^2)\varepsilon_1=0 \tag{9b}$$

for the t^0 and t^1 coefficients, respectively. Now Eq. (8a) is used to determine ε_1 in terms of the initial envelope function, u_0, the second derivative of ε_1 is calculated by differentiation of Eq. (8a), and the derivatives of u_0 are eliminated

by use of Eq. (9a) and its first integral. Substitution of g, ψ_1, ε_1, and ε_{1xx} into Eq. (9b) then results in a polynomial in u_0 with terms the order of u_0^2, u_0^4, and u_0^6. All of the previous equations will be satisfied to first order in t if the coefficients of these powers in this polynomial are equated to zero giving the set of three equations,

$$a_2\alpha^2+a_1\alpha+2\alpha^2\alpha_2\alpha_2+3a_1\alpha_2\alpha+a_1^2-8a_0=0, \tag{10a}$$

$$16\alpha\beta a_2^2+12\alpha\beta a_2+8a_1a_2\beta-2Q\alpha a_2-Qa_1-4Q\alpha - 16a_1\beta-14ND=0, \tag{10b}$$

$$-\frac{28}{3}a_2\beta^3+\left(\frac{23}{3}Q-2Qa_2\right)\beta^2+\frac{10}{3}Q^2\beta=0, \tag{10c}$$

for exponents 2, 4, and 6, respectively.

In order to determine the unknown constants in Eqs. (10) assumptions about the initial pulse shape are made. To simplify the following calculations, it is assumed that the initial pulse has a sech form, which implies that the coefficient of u_0^5 in Eq. (9a) is zero. This gives the following value for the parameter a_2:

$$a^2=\frac{Q}{2\beta}+\frac{Q^2}{4\beta^2} \tag{11}$$

in terms of the other unknown parameter, β. The value of β is easily obtained by substitution of Eq. (11) into Eq. (10c) resulting in

$$\frac{Q}{\beta}=\pm\sqrt{3}, \tag{12}$$

and Eq. (10b) finally gives an expression relating the other two parameters,

$$\frac{\alpha_2 Q}{2}(25+10\sqrt{3})+\frac{a_1 Q}{\sqrt{3}}(3\sqrt{3}-10)-14ND=0. \tag{13}$$

These steps leave a free parameter that can eventually be related to an experimental quantity such as the pulse amplitude, which is done using the definite form for u_0 after integration of Eq. (9a) yielding the initial pulse

$$u_0=\varphi_0\cosh^{-1}\left(\varphi_0\sqrt{\frac{-n}{2}}x\right), \tag{14}$$

where the effective nonlinear coefficient is $n=2N/D+2\beta a_1/D^2$, and φ_0 is the pulse amplitude. Furthermore, using this initial solution it can be shown that the parameter a_0 is related to the amplitude by the expression

$$a_0=-\tfrac{1}{4}nD^2\varphi_0^2. \tag{15}$$

Now all parameters can be evaluated in terms of the coefficients in the HONLS equation. Here it is remarked that all coefficients in the HONLS equation will be chosen so that the amplitude-dependent terms resulting from Eq. (15) will be negligible, and later this will be shown to indeed be the case. Using Eqs. (11)–(13) and (15) we obtain $\alpha_2=0.251ND/Q$ and $a_1=-0.307ND/Q$ to get the following effective nonlinear coefficient:

$$n=1.65\frac{N}{D}. \tag{16}$$

These results are combined to get a first-order time-dependent solution of the HONLS equation which will be used to determine the shape evolution of a pulse owing to the self-steepening term in the HONLS equation. The time-dependent contribution can now be obtained from Eq. (8a) for ε_1 together with the other parameters that were determined. Using the initial pulse in Eq. (14), the following pulse shape is obtained:

$$u(x,t)=\varphi_0\cosh^{-1}(\zeta x)+\left[1.05Q\sqrt{\frac{-N}{D}}\varphi_0^4\cosh^{-4}(\zeta x) \times\tanh(\zeta x)\tanh(\zeta x)\right]t, \tag{17}$$

where $\zeta=\varphi_0\sqrt{-n/2}$ is the inverse width of the initial pulse. In principle, higher-order corrections can be found using ε_2 estimated from Eq. (8b); however, the simple functions that we chose for g and $A(\psi)$ will no longer be sufficient to satisfy the second-order terms in all three equations. This is because there will not be an adequate number of free parameters to separately equate all of the powers of u_0 to zero, and one must use more complicated functions involving more parameters, or require that the coefficients in the HONLS equation have restricted values. In order to sidestep this difficulty, we will only apply Eq. (17) in the time interval where it will be a valid approximation. To determine this interval, first the magnitude of the second-order term is estimated. Using Eq. (8b) together with the previous results, it can be shown that this term is the order of

$$\varepsilon_2\approx\frac{NQ^2}{D}\varphi_0^6,$$

and comparison of this with the first-order term in Eq. (17) we obtain the inequality

$$t<\frac{D}{NQ\varphi_0^2}\sqrt{\frac{-N}{D}}, \tag{18}$$

giving a relation to be satisfied by the propagation time and the pulse amplitude.

III. SOLITON EVOLUTION

In this section typical parameters applicable to YIG films will be used to calculate the pulse shape as a function of time. Bright solitons in these systems can be formed when operation of the delay line is in the so-called magnetostatic backward volume wave configuration. In this case an external magnetic field is applied tangent to the film plane, and the pulse propagates in the direction of the applied field. Using the magnetostatic wave dispersion relation it is pos-

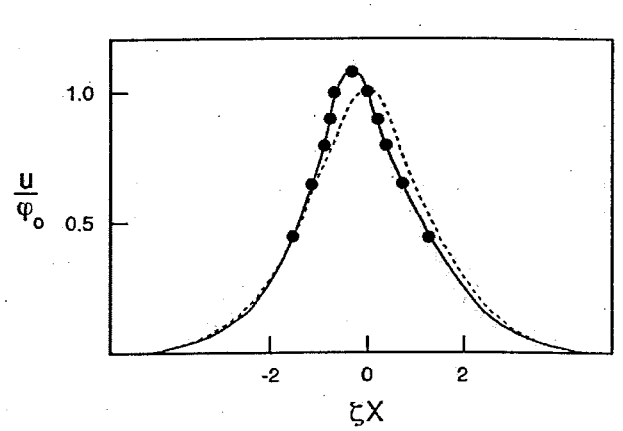

FIG. 1. Pulse shape at two different times. The dashed curve is the initial symmetric pulse, and the solid curve is the pulse after a propagation time of 80 ns. The solid points are numerical results corresponding to a propagation time of 200 ns.

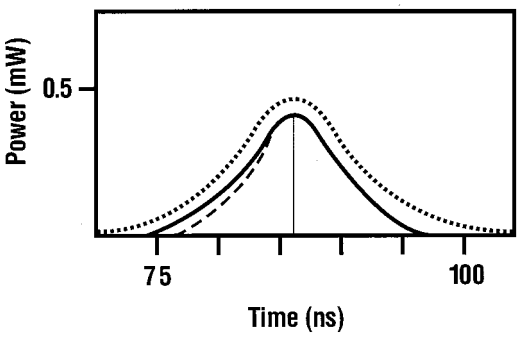

FIG. 2. Experimental pulse (solid curve) propagating in YIG film. Calculated pulse (dashed curve) formed from symmetric pulse after a propagation time of 50 ns. The relative amplitudes have been shifted slightly to better distinguish between the two pulses, and a symmetric pulse is shown by the dashed curve extending from the experimental pulse peak.

sible to calculate the dispersion parameter and the nonlinear coefficient for specific values of the carrier wave number and film thickness. This has already been done in the literature[1] so only typical values will be given here. It is more difficult to get a reliable estimate of the self-steepening coefficient, but if the k dependence of the nonlinear coefficient is known, the value of Q can be estimated from the k derivative evaluated at the carrier wave number. For one of the most recent calculations[19] of $N(k)$ it can be shown that Q is the order of 10^6-10^7, but this parameter is very dependent on the model used. To obtain numerical results giving the pulse shape versus time from Eq. (17) we will use the parameter values for a film of thickness 7.5 μm in a 1150-Oe external field giving $D=1.4\times10^3$ cm^2/s, $N=-7\times10^9$ s^{-1}, a typical value for the magnitude of the group velocity is $v_g=3.5\times10^6$ cm/s. A reasonable estimate for the self-steepening coefficient is $Q=5\times10^6$ cm/s, although it might be better to determine Q by fitting the above equation to experimental pulse shapes. Another parameter that is unknown is the initial pulse amplitude, but in order for the cubic NLS approximation to be valid this has to be small. In the following we take $\varphi_0=0.06$.

In a typical experimental setup the pulse propagates a few millimeters down the film, which corresponds to a propagation time of about 100 ns. Therefore in the following we will calculate the pulse shape for times up to about 100 ns, which is also in the neighborhood of the limiting value of time given by Eq. (18). The time development of a pulse is illustrated in Fig. 1 where Eq. (17) was used to calculate the pulse shape as a function of time using the above parameters. Both the initial and the pulse after a propagation time of about 80 ns are plotted as a function of position. Here we can clearly notice the growth of the pulse asymmetry as the pulse propagates from the initial symmetric pulse to the asymmetric pulse. The propagation of a similar initial pulse has also been numerically modeled by Eq. (1) and these results are indicated by the data points in Fig. 1. In general the numerical modeling shows that after a long propagation time (200 ns) the initial symmetric pulse will evolve into a stable asymmetric pulse, and referring to Fig. 1 it is noticed that these long propagation time numerical results almost coincide with the analytical results. The main point here is that the numerical results are qualitatively similar to the analytical results in Fig. 1 indicating that the analytical and numerical data are consistent and the analytic series solution is a good approximation. Next the temporal region where the approximations are valid is determined by using the values of the parameters in Eq. (18) giving a range of about $t<100$ ns. Since the propagation time used in Fig. 1 is close to this limit, it is expected that the larger times used in Eq. (17) will not give an accurate pulse shape. Indeed, when larger time values are used a shoulder and a secondary peak will form on the right side of the pulse. Since this is not a result of physical significance, the pulse profiles at larger values of the time are not illustrated in Fig. 1. It is finally remarked that the asymmetric pulses in Fig. 1 are similar to the initial stages of shock development in Refs. 13 and 14 which were, however, shown to be incorrect.

Finally, the pulse shape calculated from Eq. (17) is compared with experimental data. To do this we use some old data[20] from a YIG film of thickness 7.5 μm operating in the magnetostatic backward volume wave configuration. In this case the parameters used earlier are still valid and they are used to obtain the pulse form. In this experimental setup the output pulse is observed at the second antenna as the output amplitude versus time. For this reason the pulse amplitude as a function of time at a fixed position is calculated, and these results are compared with experimental data. In Fig. 2 the solid curve indicates a pulse from Ref. 20 after propagation in YIG for a time of about 80 ns. In the original experiment this pulse was formed from a 0.01-W rectangular pulse of duration 13 ns. Here notice the asymmetry of the pulse. This asymmetry seems to be a characteristic of other small amplitude pulses, maybe because it is more noticeable if the amplitude is small. Furthermore, if the pulse amplitude increases to the two-soliton threshold, the multisoliton structure has a significant effect on the pulse shape and Eq. (17) is no longer expected to be applicable. Since the experimental pulse has formed from a rectangular pulse, and a

short time is required for the pulse to evolve into a sech-type shape, the propagation time used to calculate the pulse shape was taken to be about 50 ns. The only unknown parameter is the pulse amplitude, which is a measure of the time-dependent magnetization relative to the saturation magnetization in YIG. For typical experimental conditions this is in the range $0.01<\varphi_0<0.1$ so we took the initial pulse amplitude to be an adjustable parameter, and the value $\varphi_0=0.06$ was used to calculate the pulse shape. The calculated pulse shape is shown as the dashed curve in Fig. 2 where the amplitude has been increased slightly to better compare the two pulses. To better show the asymmetry of the experimental pulse a symmetric shape is extended as a dashed curve from the pulse peak. These parameters give a good qualitative agreement between the calculated time dependence and experimental results. In conclusion, both analytical calculations and numerical simulations have shown that nonlinear dispersion in the NLS equation is one possible explanation of the asymmetry of envelope solitons propagating in YIG films.

ACKNOWLEDGMENTS

The authors acknowledge support by the National Science Foundation Grant number DMR-9972507.

[1] M. Chen, M. A. Tsankov, J. M. Nash, and C. E. Patton, Phys. Rev. B **49**, 12 773 (1994).
[2] H. Y. Zhang, P. Kabos, H. Xia, R. A. Staudinger, P. A. Kolodin, and C. E. Patton, J. Appl. Phys. **84**, 3776 (1998).
[3] C. E. Patton, P. Kabos, H. Xia, P. A. Kolodin, H. Y. Zhang, H. Staudinger, B. A. Kalinikos, and N. G. Kovshikov, J. Magn. Soc. Jpn. **23**, 605 (1999).
[4] V. E. Zakharov and A. B. Shabat, Zh. Eksp. Teor. Fiz. **61**, 118 (1972) [Sov. Phys. JETP **34**, 62 (1972)].
[5] A. N. Slavin, Phys. Rev. Lett. **77**, 4644 (1996).
[6] H. Xia, P. Kabos, C. E. Patton, and H. E. Ensle, Phys. Rev. B **55**, 15 018 (1997).
[7] V. E. Zakharov and E. A. Kuznetsov, Zh. Eksp. Teor. Fiz. **113** 1892 (1998) [JETP **86**, 1035 (1998)].
[8] N. Sasa and J. Satsuma, J. Phys. Soc. Jpn. **60**, 409 (1991).
[9] K. Porsezian and K. Nakkeeran, Phys. Rev. Lett. **76**, 3955 (1996).
[10] M. Gedalin, T. C. Scott, and Y. B. Band, Phys. Rev. Lett. **78**, 448 (1997).
[11] E. M. Gromov and V. V. Tyutin, Wave Motion **28**, 13 (1998).
[12] D. Anderson and S. Lisak, Phys. Rev. A **27**, 1393 (1983).
[13] J. R. de Oliveira and M. A. de Moura, Phys. Rev. E **57**, 4751 (1998).
[14] C. E. Zaspel, Phys. Rev. Lett. **82**, 723 (1999).
[15] Q-Han Park and S. H. Han, Phys. Rev. Lett. **84**, 3732 (2000).
[16] E. M. Gromov, L. V. Piskunova, and V. V. Tyutin, Phys. Lett. A **256**, 153 (1999).
[17] E. M. Gromov and V. I. Talanov, Chaos **10**, 551 (2000).
[18] C. E. Zaspel, P. Kabos, H. Xia, H. Y. Zhang, and C. E. Patton, J. Appl. Phys. **85**, 8307 (1999).
[19] A. N. Slavin and I. V. Rojdestvenski, IEEE Trans. Magn. **30**, 37 (1994).
[20] H. Xia, P. Kabos, R. A. Staudinger, C. E. Patton, and A. N. Slavin, Phys. Rev. B **58**, 2708 (1998).